



# Insights into the c-Jun N-terminal kinase 3 (JNK3) inhibitors: CoMFA, CoMSIA analyses and molecular docking studies

Yanda Liu<sup>1</sup> · Yewei Xie<sup>2</sup> · Yuanyuan Liu<sup>1</sup> · Pengcheng Wang<sup>1</sup> · Jiayi Ye<sup>1</sup> · Yalun Su<sup>1</sup> · Zhihong Liang<sup>1</sup> · Zhaohui He<sup>3</sup> · Haibo Zhou<sup>1</sup> · Guochao Liao<sup>2</sup> · Jun Xu<sup>1</sup> · Yiqun Chang<sup>1</sup> · Pinghua Sun<sup>1</sup>

Received: 4 February 2019 / Accepted: 1 August 2019 / Published online: 13 August 2019  
© Springer Science+Business Media, LLC, part of Springer Nature 2019

## Abstract

JNK3, a protein kinase of the MAPK family that is potently activated by a variety of environmental stress and pro-inflammatory cytokines, has been recognized as an important therapeutic target for several neurodegenerative diseases. However, due to the long development cycle and the cost of R&D, no related drugs have been released. By applying the CoMFA and CoMSIA methods, QSAR models that explore the structure-activity relationship of the JNK3 inhibitors are established and validated, the parameters are satisfactory ( $q^2 = 0.774$ ,  $r^2 = 0.991$  for CoMFA model and  $q^2 = 0.666$ ,  $r^2 = 0.990$  for CoMSIA model) and base on which a series of novel molecules are designed. Molecular docking is conducted to verify the potential of the new compounds, the results shows promising activity. We speculated that the series of compounds **S1–S11** might have some therapeutic activity in the c-jnk3 pathway, particularly the “**S8**” may prove to be the best one, which provided useful guidance for the design of new and efficient subtype selective JNK3 inhibitors.

**Keywords** JNK3 · Potential inhibitory activity · QSAR · Molecular docking

## Introduction

As a member of the mitogen-activated protein kinase (MAPK) family, the c-Jun N-terminal kinases (JNKs) regulate the serine/threonine phosphorylation of several

transcription factors when activated by various stimuli such as oxidative stress, neurotoxins, cytokines, and fatty acids (Zheng et al. 2014). JNK protein plays a dual regulatory role in cell apoptosis, and stimulation of different source types, background and subtypes of JNK will make JNK play a different role: to promote cell apoptosis or inhibit cell apoptosis (Gupta et al. 1996). There are three kinds of Human source JNK isoforms: JNK1, JNK2, and JNK3 (Chambers et al. 2013; Dérijard et al. 1994; Hibi et al. 1993; Mohit et al. 1995). JNK1 and JNK2 are omnipresence in most tissues. Recent studies showed that JNK1 and JNK2 play an important role in the development of diabetes, obesity, arthritis, cancer, and heart disease (Kyriakis et al. 1994). Inhibition of JNK1 involved in the development of obesity induced insulin resistance might be an effective way of treating type-2 diabetes. Recent studies have reported that inhibition of the abnormal activation of the JNK3 pathway can protect DA neurons and thus be used in the treatment of Parkinson's disease (Chambers et al. 2011; Kamenecka et al. 2009). JNK can directly phosphorylate epithelial cadherin 1 (E-cadherin 1, CDH1) gene in the G2 period and early mitosis, change its subcellular localization, and activate the anaphase promoting complex (anaphase-promoting complex or cyclosome, APC/C) where APC/C is the ability (Cervigni et al. 2015; Gutierrez et al. 2010),

These authors contributed equally: Yanda Liu, Yewei Xie

✉ Yiqun Chang  
changyiqun\_4907@126.com

✉ Pinghua Sun  
tsunph@jnu.edu.cn

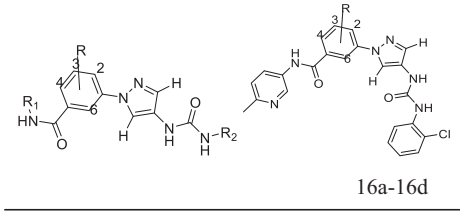
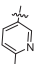

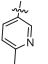
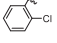
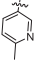
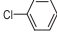
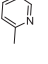
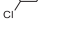
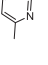

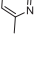
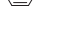
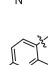
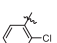
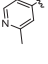
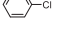
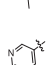
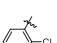
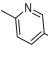
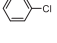
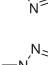
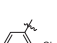
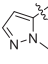
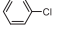
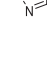




<sup>1</sup> International Cooperative Laboratory of Traditional Chinese Medicine Modernization and Innovative Drug Development of Chinese Ministry of Education, College of Pharmacy, Jinan University, Guangzhou 510632, P. R. China

<sup>2</sup> International Institute for Translational Chinese Medicine, Guangzhou University of Chinese Medicine, Guangdong, Guangzhou 510006, China

<sup>3</sup> International Research Center of Medicinal Administration, Peking University, Beijing 100191, P. R. China

<sup>4</sup> Faculty of Medicine and Health, the University of Sydney, Sydney, NSW 2006, Australia

**Table 1** The structures and activity of the molecules

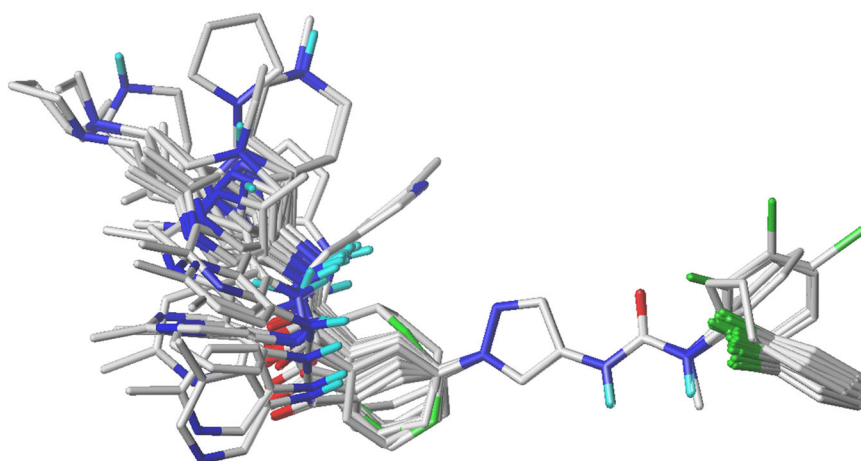
Compd.	pIC <sub>50</sub>	Main Core		Predicted Activity (CoMFA)	Residual	Predicted Activity (CoMSIA)	Residual
		R <sup>1</sup>	R <sup>2</sup>				
 16a-16d							
		R <sup>1</sup>	R <sup>2</sup>				
8b	6.939			6.939	-0.480	6.306	0.633
8c2	7.420			8.215	0.794	7.201	0.219
8d	6.225			6.303	0.079	6.279	-0.054
8e	5.738			5.802	0.065	5.958	-0.220
8f	6.504			6.434	-0.070	6.312	0.192
8j	5.514			5.445	-0.069	5.440	0.074
22b	6.851			6.877	0.026	6.873	-0.022
22c	6.851			6.815	-0.036	6.805	0.045
22f	7.009			6.990	-0.018	7.004	0.005
22g	6.886			6.887	0.001	6.904	-0.018
22h	7.208			7.279	0.071	7.259	-0.052
22i	6.507			7.175	0.668	7.105	-0.598
26a	6.876			6.886	0.010	6.885	-0.009
26b	6.693			7.193	0.501	6.909	-0.217
26c	6.790			6.784	-0.006	6.743	0.048
26d	6.936			7.375	0.440	7.062	-0.127

26f	6.943		7.063	0.119	7.076	-0.132	
26g	7.469		7.549	0.081	7.525	-0.056	
26h	7.678		7.695	0.017	7.577	0.101	
26i	7.638		7.564	-0.074	7.576	0.062	
26j	7.638		7.565	-0.073	7.565	0.074	
26l	6.863		6.857	-0.006	6.941	-0.078	
26m	7.000		6.958	-0.042	6.972	0.028	
26n	6.686		6.732	0.046	6.740	-0.054	
26o	6.772		6.662	-0.110	6.727	0.045	
26p	7.469		7.475	0.007	7.551	-0.082	
26q	7.538		7.504	-0.033	7.535	0.002	
SR-4326	6.932		6.932	0.000	6.927	0.005	
16a	7.097	/	2-F	7.152	0.055	7.073	0.024
16b	5.338	/	3-F	5.370	0.031	5.305	0.034
16c	7.149	/	4-F	7.113	-0.036	7.106	0.043
16d	6.638	/	6-F	6.605	-0.034	6.642	-0.003

which deduced that JNK is involved in the regulation of cell cycle by indirect interaction with CDH1. The selective expression of JNK3 primarily in the brain along with findings that JNK3 knockout mice exhibit amelioration in animal models of Parkinson and Alzheimer's disease (Chambers et al. 2011), makes the inhibition of this isoform a particularly promising therapeutic target for these degenerative diseases.

Currently, the research on inhibitors of c-jnk3 series is not clear due to the uncertainty of clinical efficacy (Ansideri et al. 2018), long period of development, high risk of the development cycle and investment funds, and the research on the mechanism of key regulation and control channels is not clear yet (Muth et al. 2017; Rech et al. 2007; Schattel

et al. 2011; Zhao et al. 2006; Kamenecka et al. 2009; Koch et al. 2014; Siddiqui and Reddy 2010). Therefore, development of JNK inhibitors as therapeutic agents has gained considerable interest over the past few years. Identifying novel and potent inhibitors of JNK3 may contribute toward not only neuroprotective therapies with reduced untoward side effect but also understanding the mechanism of the therapy. Some achievements have been obtained by researchers from many groups (Li et al. 2017; Qin et al. 2013; Lange et al. 2015) among which a series of aminopyrazole derivatives drew our attention (Zheng et al. 2014). We believed that with the information based on the previous study and the developing CADD technology, further research that leads to more potent compounds could be

**Fig. 1** Alignment of all compounds**Table 2** Statistical results of CoMFA and CoMSIA models

PLS statistics	CoMFA	CoMSIA
$q^2$	0.774	0.666
$r^2$	0.991	0.990
S	0.064	0.069
F	373.511	322.699
$r^2_{\text{bootstrap}}$	0.996	0.998
$S_{\text{bootstrap}}$	0.039	0.032
Optimal components	5	5
<i>Field distribution</i>		
Steric	0.600	0.194
Electrostatic	0.400	0.340
Hydrophobic		0.321
Hydrogen bond donor		0.145
$r^2_{\text{pred}}$	0.995	0.996

established. The novel simulation methods are more credible in studying the structure-activity relationships, which can greatly reduce time and cost consuming in the early stage, and significantly increase the efficiency (Sharma and Ghoshal 2006; Buckingham et al. 1995; Dorsey et al. 1994). Thus the QSAR and molecular docking are introduced into our work to help us get the insight into the inhibitors of c-jnk3.

## Methodology

All molecular structure modeling and statistical analysis are performed on SYBYL-X 2.0 software (Tripos, Inc., St. Louis, MO, USA), and the default parameters are used in the following calculations unless otherwise specified.

## Dataset

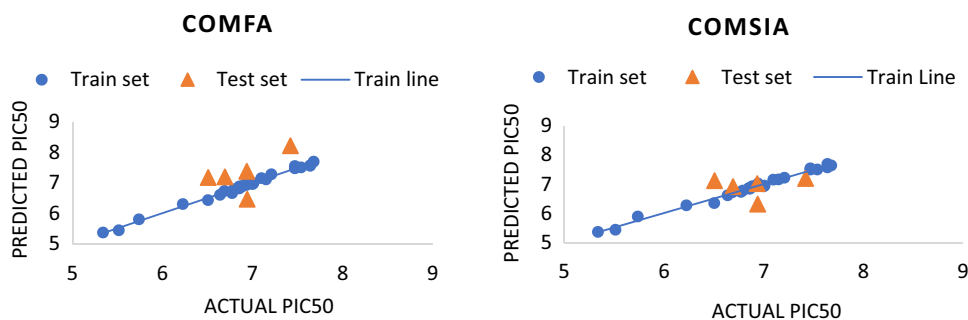
The compound structures and biological data are collected from the lectures (Zheng et al. 2014). The 3D structures of compounds are sketched using SYBYL-X, and conjugate gradient methods was applied when conducting the energy minimization under the conditions of a gradient convergence of 0.05 kcal in Gasteiger-Hückel charge. All these data forms are shown in Table 1. Compounds **22i**, **26b**, **26d**, **8b**, and **8c2** are selected as the test set randomly, and all other compounds constitute the training sets.

## QSAR model

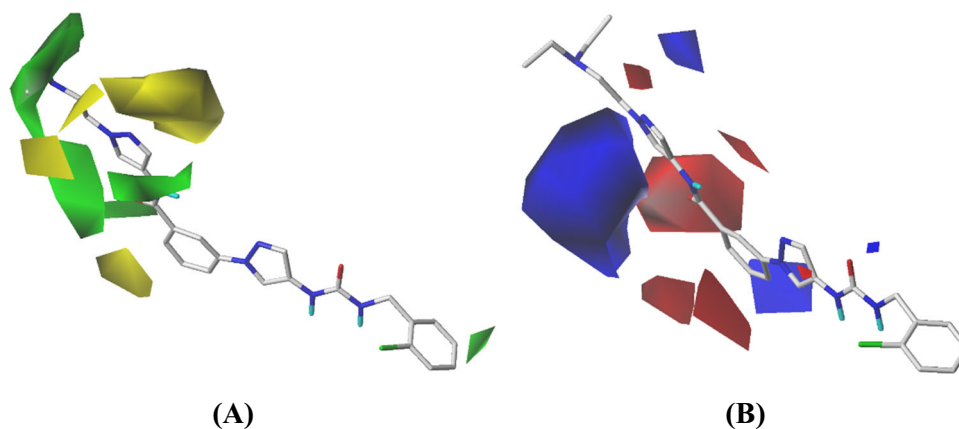
Molecular alignment is a key factor affecting CoMFA and CoMSIA model results. Because all compounds have a common structure of N-(6-methylpyridin-3-yl)-3-(4-(3-phenylureido)-1H-pyrazol-1-yl) benzamide, we treat it as the core substructure in the alignment. With the highest activity compound **26h** used as template molecule, other 32 compounds are superimposed with an energy convergence criteria for 0.21 kJ/mol-Å. The alignment of all compounds is shown in Fig. 1 where we can see all molecules are well overlapped.

A three-dimensional cube with the step size of 1 and 4 Å beyond the boundary of aligned compounds in every direction was introduced to calculate the descriptors of CoMFA and CoMSIA (Huang et al. 2001). As to the CoMFA (Srivastava et al. 2008), a probe (a  $sp^3$  C atom with 1e charge) is generated to compute both the electrostatic and steric fields, where the values of energy were cut under 30 kcal/mol (Xiao et al. 2008). As a CoMFA's extension, CoMSIA method, with three more fields (hydrophobic, h-bond acceptor and h-bond donor), were calculated by an atomic probe with 1.0 Å radius and  $\delta 1.0$  charge. Default value of attenuation factor of 0.3 was applied in the modeling (Klebe and Abraham 1999). The correlation of

**Fig. 2** Graph of actual versus predicted  $\text{pIC}_{50}$  of the training set and the test set using CoMFA and CoMSIA



### Contour map analysis



**Fig. 3** Coeff contour maps of CoMFA analysis. **a** Sterics; **b** electrostatics

CoMFA and CoMSIA fields to the biodata were computed by the PLS (Partial least squares) method (Chambers et al. 2013). Leave-one-out analysis, where every molecule will be extracted from the database once and their biological value will be predicted based on the model derived from the rest of the compounds, was conducted to calculate the cross-validated  $q^2$ . In order to further verify the prediction capacity, a parameter of the predictive correlation coefficient ( $r^2_{\text{pred}}$ ) is calculated (Wang et al. 2016).

### Docking analysis

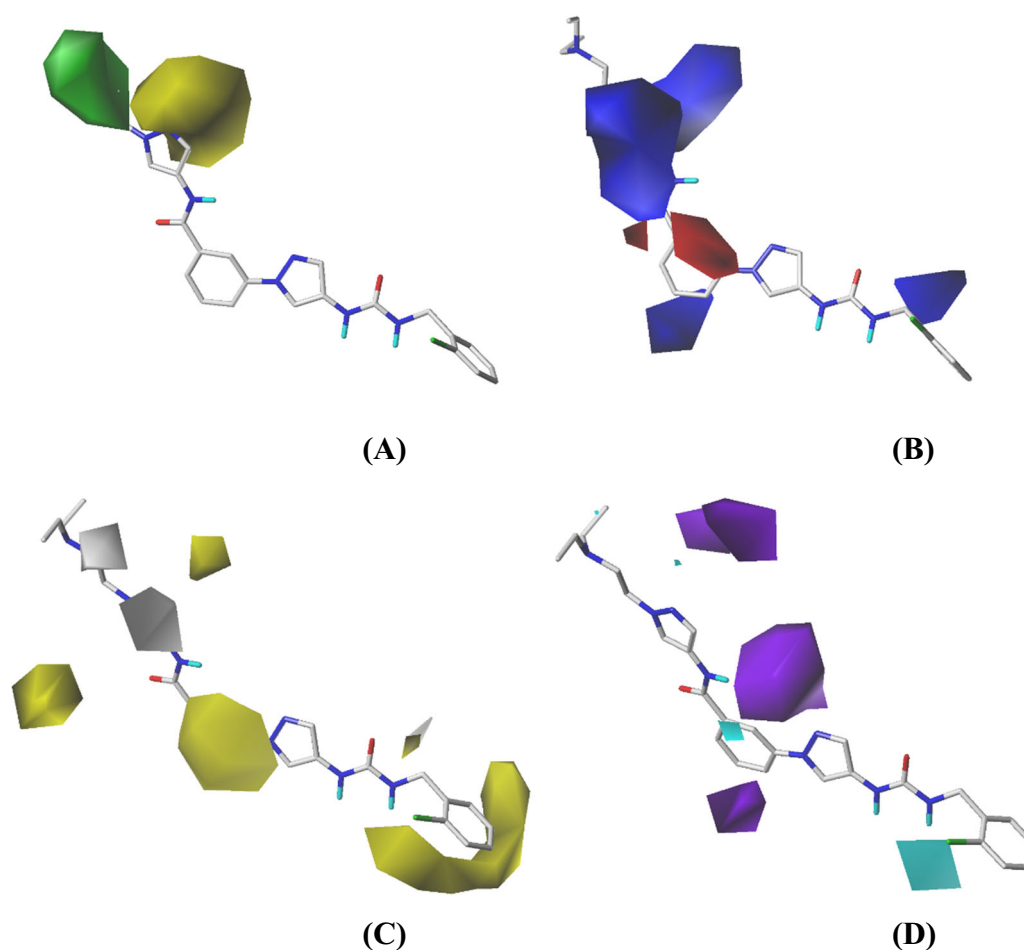
Surflex-Dock in SYBYL-X was applied to study molecular docking in this work using a patented search engine and an empirical scoring function to dock ligands into a protein's binding site (Jain 2003). The crystal structure of JNK3 was downloaded from the RCSB Protein Data Bank (PDB ID: 3TTI) (Krenitsky et al. 2012). After the preparation of the protein, our designed compounds are docked into the binding pocket. The total scores of Surflex-Dock representing binding affinities are expressed in the logarithm of the  $K_d$  value. The results were compared with the scores of

current ligand to explore the credibility and validation of the model.

## Results and discussion

### CoMFA and CoMSIA results

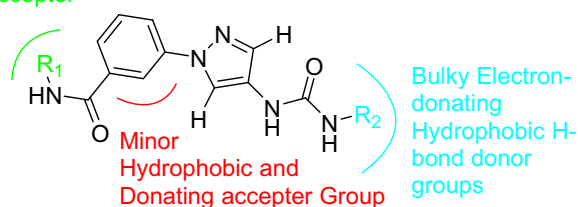
The training set was constituted by 32 compounds with a wide range of  $\text{pIC}_{50}$  (5.00–8.00). The CoMFA obtained from the training set return us good parameters: the  $q^2$  (cross-validated correlation coefficient), with an ONC of 6, is 0.774 ( $>0.6$ ); the  $r^2$  is 0.991 and STD is 0.064; F value and  $r^2_{\text{pred}}$  are also satisfactory as 373.511 and 0.995, respectively. The electrostatic field contributes 0.400 while steric fields contributes 0.600. As to CoMSIA, with three extra fields than CoMFA, several models were carried out, among which the best one consisted with four kinds of fields (steric, electrostatic, hydrophobic H-bond donor) gave us satisfactory results: the  $q^2$  of 0.666 ( $>0.6$ ) and  $r^2$  of 0.990 with 6 optimized number of components; a good STD of 0.069, F value of 322.699, and  $r^2_{\text{pred}}$  of 0.996. The contributions of four fields were 0.194, 0.340, 0.321, and



**Fig. 4** The coeff contour maps of CoMSIA analysis. **a** Sterics; **b** electrostatics; **c** hydrophobic; **d** donor

**Fig. 5** Structure–activity relationships resulted from present research

Bulky, Electron-donating, hydrophobic and H-bond acceptor groups favored.



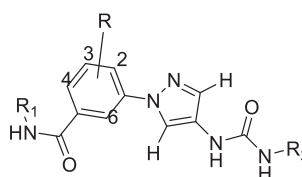
0.145, respectively. The parameters of the models were shown in Table 2, and the statistics indicated that the CoMFA and CoMSIA models are capable in predicting the activities of the derivatives (Fig. 2).

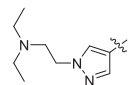
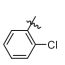
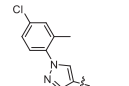
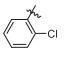
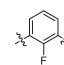
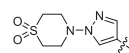
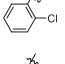
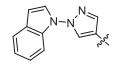
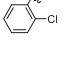
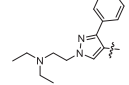
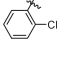
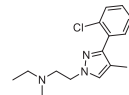
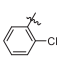
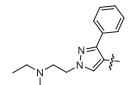
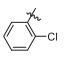
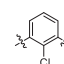
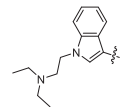
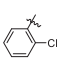
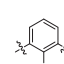
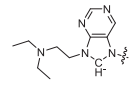
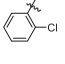
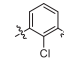
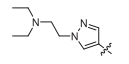
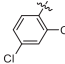
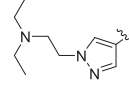
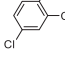
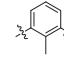
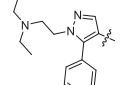
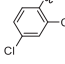
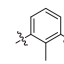
### Contour map analysis

CoMFA Contour map in Fig. 3 depicted the CoMFA steric and electrostatic contour plots for the most active compound **26h**. The green and yellow blocks in Fig. 3a indicated steric favorable and unfavorable locations, respectively. Similarly,

blue and red blocks in Fig. 3b, respectively, represented the electron donating and withdrawing sites.

As shown in Fig. 3a, the large green contour near  $R_1$  indicated where a bulky group would benefit to the activity, which can explain the higher activity of molecular **26g**, **26h**, **26i**, and **26j** than **26a**, **26b**, and **26c** whose substitutes are spatially smaller. A small yellow contour around benzene ring suggested that a minor substituent at this location might be better. The small green contour near  $R_2$  represent a larger substituents at this site would be favored.

**Table 3** Structures and predicted pIC<sub>50</sub> values of newly designed molecules


Molecule	Substituent			Predicted pIC <sub>50</sub>	
	R1	R2	R	CoMFA	CoMISA
26h			/	7.695	7.577
S1				6.593	6.530
S2			/	7.167	7.080
S3			/	7.178	6.922
S4			/	6.718	6.667
S5			/	6.713	6.565
S6				6.695	6.508
S7				6.683	6.683
S8				7.196	6.777
S9			/	7.277	7.175
S10				6.881	7.055
S11				6.902	6.792

In Fig. 3b, the blue and red denoted regions which were favored and disfavored, respectively. The large blue contour above R<sub>1</sub> indicated that electron-donating groups at this site would be beneficial. The blue contour close to the point of the benzene ring site also advise us that electron-donating

groups at this site may be helpful in improving the activity. Another red contour near the carbonyl revealed electron-donating groups at this position was detrimental to the potency.

With the compound **26h** still as the template molecule, the CoMISA contours maps were shown in Fig. 4. Figure 4a, b depicted the steric and electrostatic contours of CoMSIA, respectively, which are similar to CoMFA ones in Fig. 3. As to the hydrophobic contours (Fig. 4c), yellow and white blocks emphasized the hydrophobic and hydrophilic favored regions, respectively. The cyan and purple blocks in H-bond donor contour maps (Fig. 4d) indicated favorable and unfavorable to H-bond donor, respectively.

Near the substituent R1, there is a blue region near the site. This indicates that if the substituent in the region is increased, the hydrophilicity will be helpful to enhance the activity, and there is also a huge yellow contour around the benzene ring position and R2 site which shows that hydrophobic groups play a large role in this region. That is why the compound **8c2** has the higher activity than **8b**.

The hydrogen bond donor contour maps of the CoMSIA model with compound **26h** were depicted in Fig. 4d. A purple contour around the R1 indicated that

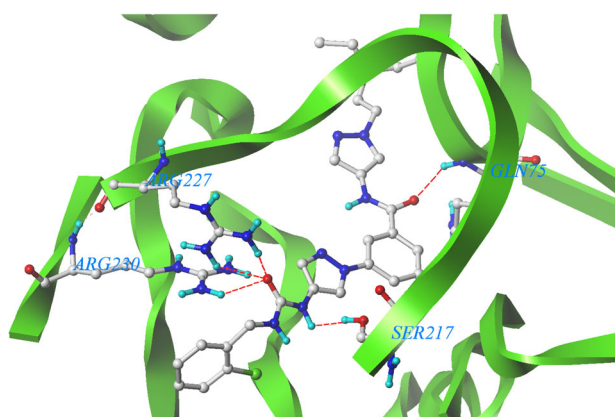


Fig. 6 Binding mode of compound **26h** in the active site

H-bond acceptor groups at this site would be harmful to the potency. This agrees with the fact that most active compounds had a non-polar methyl group at this site which could not form a H-bond with the CLC chloride channel receptor. As seen from Fig. 4d, the large purple contour above the benzene ring site, suggesting that a H-bond acceptor group at this site would be favorable. A cyan contour near the R2 showed that a H-bond donor at this site may benefit the potency. This also consisted with the observations that **8c2** (acting as H-bond donor) compounds showed stronger inhibitory activities than **8b**.

### Summary of the structure-activity relationships

The structure-activity relationships revealed by the present study were summarized in Fig. 5. The bulky, electron-withdrawing and steric groups at R<sub>1</sub> are crucial to enhance the activity, on the other hand, the bulky and hydrophobic groups to R<sub>2</sub> may improve the potency. By introducing electron-donating groups to the *meta*-position of R<sub>1</sub> may also be beneficial to the activity. In addition, the hydrogen donor was also preferred in the red zone.

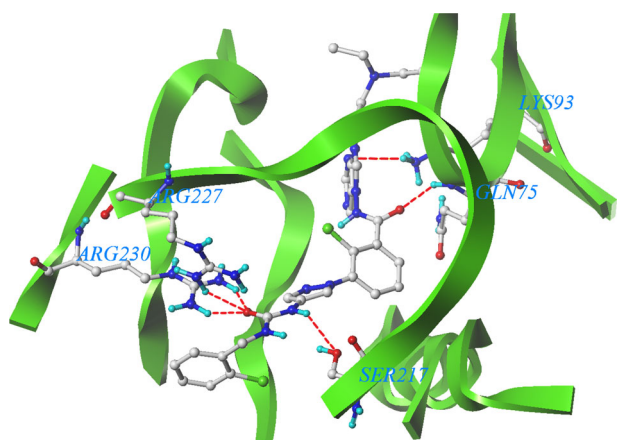
### Designing novel derivatives

Based on QSAR revealed by this study above, we selected compound **26h** (PIC<sub>50</sub> = 7.678) as lead compound, and 11 new potent molecules (S1–S11) were designed. These molecules were superposed to the alignment as the test set, then their activities on JNK-3 inhibition were calculated using 3D-QSAR models we built previously. The chemical structures as well as calculated activities are demonstrated in Table 3.

Table 4 Compounds S1–S11 docking with Jnk3 (PDB code 3TTI) scoring function

Name	Total_Score	Crash	Polar	D_Score	PMF_Score	G_Score	ChemScore	CScore	Global_CScore
S8_3TTI	9.1773	-2.5984	2.8066	-213.7009	-71.7903	-317.2268	-22.072	5	5
S7_3TTI	8.6264	-2.8382	2.6037	-172.3271	-24.156	-296.696	-29.6981	4	5
S11_3TTI	8.4897	-1.5667	0.7321	-162.9011	0.2982	-295.748	-20.8738	2	3
S5_3TTI	7.8356	-3.4863	0.0908	-168.2548	-25.3534	-331.9766	-25.7823	3	5
S4_3TTI	7.2454	-1.7299	0.4529	-164.4211	-6.5733	-274.8212	-22.9023	5	4
S3_3TTI	6.933	-1.251	2.5327	-129.1543	-38.4155	-260.7178	-22.6051	4	4
S9_3TTI	6.444	-1.8628	1.4257	-156.7623	-18.0862	-260.6376	-22.6443	4	5
S10_3TTI	6.3657	-1.3441	1.1449	-132.6239	-25.3717	-224.5537	-21.7397	4	4
26h_3TTI	5.8952	-3.4993	1.568	-153.6369	-35.3367	-291.1491	-23.2502	5	5
S6_3TTI	5.5913	-1.4618	0.9993	-145.6335	-8.6134	-242.3757	-21.349	1	2
S1_3TTI	5.43	-1.8817	2.8509	-120.6864	-37.1271	-195.6978	-22.3291	3	4
S2_3TTI	4.145	-2.9707	0.0795	-148.606	-30.4808	-269.7304	-19.7032	4	3





**Fig. 7** H-bond between compound **S8** and residues in the binding pocket

### Molecular docking analysis

Figure 6 showed the docking pose of compound **26h** in JNK3 (Koch et al. 2014). The hydroxyl groups acted as hydrogen bond donor and acceptor by forming a H-bond with Gln75 and Arg227-Arg230, respectively, matching the corresponding CoMSIA hydrogen bond donor and acceptor contour maps. Moreover, a cavity located beneath the pyrazol ring where steric contour map hints us a bulky group favored verified our results. The reason why the molecule **26h** showed higher docking score than most other structures may commentate in following results. As shown in Fig. 6, 3-NH on the side chain R1 of **26h** formed H-bond with the carbonyl group of Arg227-Arg230. Main core 4 carbonyl of **26h** formed H-bond with the -NH group of Gln75. The formation of hydrogen bonds with key amino acid groups may also explain the reason why **26h** is higher than other structures and the chlorobenzene group in the end region exerts force against the strong molecules of the docking protein. The detail review of docking results proves the binding effects of **26h** are stronger than that of the most other structures on C-JNK3 Protein, further speculating JNK3 (3TTI) is the target of prediction for compound **26h** groups with active pockets of C-JNK3 inhibitors.

With the same parameter that we optimized to dock the compound **26h**, the designed compounds, **S1–S11**, were also placed into the receptor. As shown in Table 4, the total score of compounds **S3**, **S4**, **S7**, **S8**, and **S9** is quite high, among which compound **S8** even showed a total score higher than 9. Despite the high total scores of compounds **S5** and **S11**, their CScore and global\_CScore which is <4 limited their approval of potency. The positive correlation of QSAR predicted activity and the docking scores of compounds **S1–S11** were verified by aligning their results. Comparing with **26h**, the reason that compound **S8** has a higher score, as shown in Fig. 7, may be due to the larger

contact area between the receptor binding pocket and substituent R1 and R2. In addition, the key hydrogen bonds between **S8** and JNK3 are quite similar but firmer than those between **26h** and JNK3, especially the H-bond between Arg227, Arg230, Gln75, and ligand showed essential all the time. The interactions and binding mode of our compounds are associated with the mechanism research of the JNK-3 dynamic study (Mishra and Günther 2018) which indicated the conformation rearrangement of hinge region caused by inhibitors may be the key factor.

### Conclusion

In this study, we have established CoMFA model ( $q^2 = 0.774$ ,  $r^2 = 0.991$ ) and CoMSIA model ( $q^2 = 0.666$ ,  $r^2 = 0.990$ ) with good correlative and predictive abilities from the c-Jun N-terminal kinase 3 (JNK3) inhibitors. The CoMFA and CoMSIA contour maps provided information to summarize the structure–activity relationship and characterize the structural features affecting the neuronal recovery activity. In addition, good prediction ability, experimental observation group compounds indicate that these models can be used to predict the accord with the  $IC_{50}$  value, and based on which, 11 new molecules are predicted to reach same or better activity. Further validation is conducted through the docking study. The results indicate that our series of compounds are promising as c-jnk3 inhibitors, suggesting that the models can be helpful for the development of discovering novel inhibitors of JNK3.

**Acknowledgements** This work was supported by the Natural Science Foundation of China (No. 81573294, 81773593, 81872759), the Excellent Young Teachers Program of Guangdong Provincial Colleges and Universities (YQ 2015061) and the Pearl River S&T Nova Program of Guangzhou (201610010100). We thank the software support from Dr. Junxia Zheng of the Guangdong University of Technology.

### Compliance with ethical standards

**Conflict of interest** The authors declare that they have no conflict of interest.

**Publisher's note:** Springer Nature remains neutral with regard to jurisdictional claims in published maps and institutional affiliations.

### References

- Ansideri F, Macedo JT, Eitel M, El-Gokha A, Zinad DS, Scarpellini C, Laufer SA (2018) Structural Optimization of a Pyridinylimidazole scaffold: shifting the selectivity from p38 $\alpha$  mitogen-activated protein kinase to c-Jun N-terminal kinase 3. *ACS Omega* 3(7):7809–7831
- Buckingham J, Glen RC, Hill AP, Hyde RM, Martin GR, Robertson AD, Woollard PM (1995) Computer-aided design and synthesis

- of 5-substituted tryptamines and their pharmacology at the 5-HT<sub>1D</sub> receptor: discovery of compounds with potential anti-migraine properties. *J Med Chem* 38(18):3566–3580
- Cervigni RI, Bonavita R, Barretta ML, Spano D, Ayala I, Nakamura N, Colanzi A (2015) JNK2 controls fragmentation of the Golgi complex and the G2/M transition through phosphorylation of GRASP65. *J Cell Sci* 128(12):2249–2260
- Chambers JW, Howard S, LoGrasso PV (2013) Blocking c-Jun N-terminal kinase (JNK) translocation to the mitochondria prevents 6-hydroxydopamine-induced toxicity in vitro and in vivo. *J Biol Chem* 288(2):1079–1087
- Chambers JW, Pachori A, Howard S, Ganno M, Hansen Jr D, Kamenecka T, Cherry L (2011) Small molecule c-jun-N-terminal kinase inhibitors protect dopaminergic neurons in a model of Parkinson's disease. *Acs Chem Neurosci* 2(4):198–206
- Dérjard B, Hibi M, Wu IH, Barrett T, Su B, Deng T, Davis RJ (1994) JNK1: a protein kinase stimulated by UV light and Ha-Ras that binds and phosphorylates the c-Jun activation domain. *Cell* 76(6):1025–1037
- Dorsey BD, Levin RB, McDaniel SL, Vacca JP, Guare JP, Darke PL, Schleif WA (1994) L-735,524: the design of a potent and orally bioavailable HIV protease inhibitor. *J Med Chem* 37(21):3443–3451
- Gupta S, Barrett T, Whitmarsh AJ, Cavanagh J, Sluss HK, Derjard B, Davis RJ (1996) Selective interaction of JNK protein kinase isoforms with transcription factors. *EMBO J* 15(11):2760–2770
- Gutierrez GJ, Tsuji T, Chen M, Jiang W, Ze'ev AR (2010) Interplay between Cdh1 and JNK activity during the cell cycle. *Nat Cell Biol* 12(7):686
- Hibi M, Lin ANNING, Smeal T, Minden A, Karin M (1993) Identification of an oncoprotein-and UV-responsive protein kinase that binds and potentiates the c-Jun activation domain. *Gene dev* 7(11):2135–2148
- Huang X, Liu T, Gu J, Luo X, Ji R, Cao Y, Jiang H (2001) 3D-QSAR model of flavonoids binding at benzodiazepine site in GABAA receptors. *J Med Chem* 44(12):1883–1891
- Jain AN (2003) Surflex: fully automatic flexible molecular docking using a molecular similarity-based search engine. *J Med Chem* 46(4):499–511
- Kamenecka T, Jiang R, Song X, Duckett D, Chen W, Ling YY, Cameron MD (2009) Synthesis, biological evaluation, X-ray structure, and pharmacokinetics of aminopyrimidine c-jun-N-terminal kinase (JNK) inhibitors. *J Med Chem* 53(1):419–431
- Klebe G, Abraham U (1999) Comparative molecular similarity index analysis (CoMSIA) to study hydrogen-bonding properties and to score combinatorial libraries. *J Comput Aid Mol Des* 13(1):1–10
- Koch P, Gehring M, Laufer SA (2014) Inhibitors of c-Jun N-terminal kinases: an update. *J Med Chem* 58(1):72–95
- Krenitsky VP, Nadolny L, Delgado M, Ayala L, Clareen SS, Hilgraf R, Wright J (2012) Discovery of CC-930, an orally active anti-fibrotic JNK inhibitor. *Bioorg Med Chem Lett* 22(3):1433–1438
- Kyriakis JM, Banerjee P, Nikolakaki E, Dai T, Rubie EA, Ahmad MF, Woodgett JR (1994) The stress-activated protein kinase sub-family of c-Jun kinases. *Nature* 369(6476):156
- Lange A, Günther M, Büttner FM, Zimmermann MO, Heidrich J, Hennig S, Koch P (2015) Targeting the gatekeeper MET146 of C-Jun N-terminal kinase 3 induces a bivalent halogen/chalcogen bond. *J Am Chem Soc* 137(46):14640–14652
- Li S, Fan J, Peng C, Chang Y, Guo L, Hou J, Xiao G (2017) New molecular insights into the tyrosyl-tRNA synthase inhibitors: CoMFA, CoMSIA analyses and molecular docking studies. *Sci Rep* 7(1):11525
- Mishra P, Günther S (2018) New insights into the structural dynamics of the kinase JNK3. *Sci Rep* 8(1):9435
- Mohit AA, Martin JH, Miller CA (1995) p493F12 kinase: a novel MAP kinase expressed in a subset of neurons in the human nervous system. *Neuron* 14(1):67–78
- Muth F, El-Gokha A, Ansideri F, Eitel M, Döring E, Sievers-Engler A, Laufer SA (2017) Tri- and tetrasubstituted pyridinylimidazoles as covalent inhibitors of c-Jun N-terminal kinase 3. *J Med Chem* 60(2):594–607
- Qin LT, Liu SS, Xiao QF, Wu QS (2013) Internal and external validations of QSAR model: Review. *Environ Chem* 32(7):1205–1211
- Rech JC, Yato M, Duckett D, Ember B, LoGrasso PV, Bergman RG, Ellman JA (2007) Synthesis of potent bicyclic bisarylimidazole c-jun N-terminal kinase inhibitors by catalytic C–H bond activation. *J Am Chem Soc* 129(3):490–491
- Schattel V, Hinselmann G, Jahn A, Zell A, Laufer S (2011) Modeling and benchmark data set for the inhibition of c-Jun N-terminal kinase-3. *J Chem Inf Model* 51(3):670–679
- Sharma P, Ghoshal N (2006) Exploration of a binding mode of benzothiazol-2-yl acetonitrile pyrimidine core based derivatives as potent c-Jun N-terminal kinase-3 inhibitors and 3D-QSAR analyses. *J Chem Inf Model* 46(4):1763–1774
- Siddiqui MA, Reddy PA (2010) Small molecule JNK (c-Jun N-terminal kinase) inhibitors. *J Med Chem* 53(8):3005–3012
- Srivastava V, Kumar A, Mishra BN, Siddiqi MI (2008) Molecular docking studies on DMDP derivatives as human DHFR inhibitors. *Bioinformation* 3(4):180
- Wang Z, Chang Y, Han Y, Liu K, Hou J, Dai C, Chen W (2016) 3D-QSAR and docking studies on 1-hydroxypyridin-2-one compounds as mutant isocitrate dehydrogenase I inhibitors. *J Mol Struct* 1123:335–343
- Xiao A, Zhang Z, An L, Xiang Y (2008) 3D-QSAR and docking studies of 3-arylquinazolinethione derivatives as selective estrogen receptor modulators. *J Mol Model* 14(2):149–159
- Zhao H, Serby MD, Xin Z, Szczepankiewicz BG, Liu M, Kosogof C, Pederson T (2006) Discovery of potent, highly selective, and orally bioavailable pyridine carboxamide c-Jun NH<sub>2</sub>-terminal kinase inhibitors. *J Med Chem* 49(15):4455–4458
- Zheng K, Iqbal S, Hernandez P, Park H, LoGrasso PV, Feng Y (2014) Design and synthesis of highly potent and isoform selective JNK3 inhibitors: SAR studies on aminopyrazole derivatives. *J Med Chem* 57(23):10013–10030